Mutual Influence of Cavity Resonances of a Shielding Enclosure on the Resonance of a Dipole inside that Enclosure

Zhao CHEN
Healthcare R&D
Barco NV
8500 Kortrijk, Belgium
zhao.chen@barco.com

Tim Claeys
ESAT-WaveCoRe, M-Group
KU Leuven Bruges Campus
8200 Bruges, Belgium
tim.claeys@kuleuven.be

Ronny Deseine
Healthcare R&D
Barco NV
8500 Kortrijk, Belgium
ronny.deseine@barco.com

Davy Pissoort
ESAT-WaveCoRe, M-Group
KU Leuven Bruges Campus
8200 Bruges, Belgium
davy.pissoort@kuleuven.be

***Abstract*— In recent years, a risk-based approach has been proposed to better manage EM-related risks of electronic systems. Within this approach it is critical to detect potential risks as much and as early as possible. Unfortunately, many hazards (potential contributors to risks) are "hiding" deep in the system and/or can only appear when "excited" under certain conditions. One such example is electromagnetic (EM) resonance of components and structures (e.g., traces, heatsinks, PCBs, enclosures) within electronic systems. These resonances can further lead to unintended and increased coupling effects which may result in seriously hazardous situations. In this paper, we consider the relatively simple but basic case of a trace (modelled as a dipole) within a closed metallic enclosure. Both quantitative calculations and full-wave EM-simulation results reveal the complexity of the possible resonance mechanisms and interactions.**

Keywords*— *EMC, EM resonance, closed enclosure, EM-related risks, risk management

I. INTRODUCTION

Due to the rapid development of electronic technologies and their use in e.g. health applications, safety of these technologies is becoming more and more crucial. One of the notable factors that may greatly affect the safety of electronic systems are EMI (Electromagnetic Interference) issues. When talking about risks which are related to EMI, one normally refers to two aspects: EM emission and EM immunity. Thus, to mitigate the EMI related risks, both aspects ought to be addressed. Some related work has been performed in the past. For example, models and methodologies have been developed to emulate and predict the electromagnetic (EM) emissions of PCBs. Also, the mechanism of coupling effects of incident EM waves on PCBs inside electronic systems was investigated [1][2].

For already quite a long time, the approach that is widely adopted by industry to manage EMI-related risks, is the "rule-based" approach. The essence of this approach is that as long as the design of electronic system/device follows certain design guidelines and passes relevant testing standards, it is assumed that EMI related risks are sufficiently managed. However, this traditional approach is not sufficient any more for today's critical applications. First, the standards or guidelines applied in "rule-based" approach, inevitably lag behind the development of electronic technology. Second, it has been proven that testing only can never guarantee the safety of a system or device [3]. To overcome the above, a new "risk-based" approach was proposed and has already caught wide attention [4][5][6]. In this approach, risk management is the essential process.

Before managing the potential risks, the hazards need to be clearly identified. However, since some of them can only show up under very specific conditions, they are often difficult to be discovered and thus can cause unexpected and incomprehensible problems during operation of the system. One example is the EM resonance of components in electronic systems. In the past, several researches have studied EM resonances [7][8][9]. These previous studies targeted EM resonances of enclosures together with apertures or slots and provided us with good views on the relationships between EM resonances and openings. However, when EM resonances are generated in an (almost) closed system, more complex influences will arise due to the interactions between the internal components and the closed enclosure. To better understand the mechanism of such interactions and accordingly to be able to identify possible resonance-related risks better upon which more appropriate mitigation measures can be taken, in this paper a simplified electronic system represented by a dipole and closed metallic box is studied. It is shown that this simple case already leads to some quite surprising results where the resonant frequency of the internal dipole deviates significantly from its value in free-space. The latter would typically be used as in estimate in current practice.

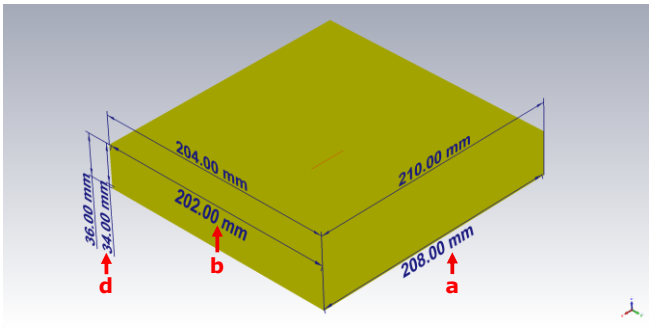

Fig. 1. Modeled electronic system (a 30 mm dipole in a closed metallic box with inner dimension of 208 mm×202 mm×34 mm).

The research leading to these results has received funding from the European Union's Horizon 2020 research and innovation programme under the Marie Skłodowska-Curie Grant Agreement No 812.790 (MSCA-ETN PETER). This publication reflects only the authors' view, exempting the European Union from any liability. Project website: http://etn-peter.eu/.

The remainder of this paper is organized as follows. In Section II, the theoretical basis of the resonance frequencies of both the dipole and the metallic enclosure is given and the calculated results are confirmed with simulations by using a full-wave EM-solver (CST Studio Suite 2020). Furthermore, in Section III, the influence on resonant frequencies, as result of the interactions between the dipole and the enclosure, is explored. Finally, the conclusions and future work are described in Section IV.

II. Resonances of the Stand-Alone Dipole and Box

To find out the interactions between the components and the enclosure of an electronic system/device, a model of such a system is modeled in a full-wave EM-solver. To simplify the analysis, our modeled system (Fig. 1) only consists of one component (a 30 mm dipole) and a closed metallic enclosure. However, as it will be shown in the next section, even for such a simplified model, the interactions can be rather complicated. Thus, instead of directly analyzing the whole electronic system, the resonances of the two separate parts, the dipole and closed metallic box, are analyzed separately. By doing this, the necessary "baselines" can be obtained and the changes due to the interactions can be figured out more easily.

A. Dipole resonance

The simplest dipole consists of two wires with equal lengths and its source in the middle. Since a dipole is usually fed exactly at its center, it is also known as a "balanced antenna" [10]. At its intrinsic resonance, the antenna will only have a real part impedance (resistance), which means that the imaginary part (reactance, caused by inductance and capacitance) vanishes at the resonant frequencies. Theoretically for a dipole antenna in free space, to be effectively resonant, it should be electrically half wavelength (0.5 λ) at its resonant frequencies. However, in practice, due to the "end effect", the actual dipole length for its first resonant frequency is slightly shorter, between 0.47 λ to 0.48 λ, depending on radius of the dipole [11]. A thinner dipole will

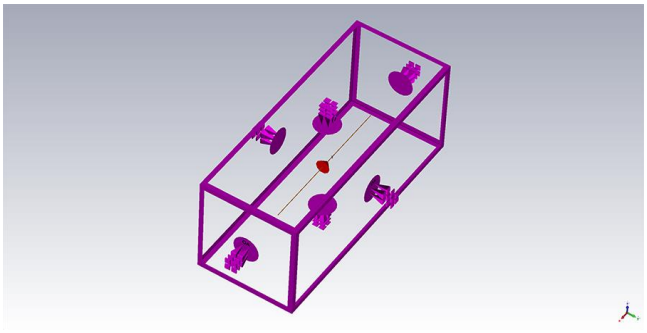

(a)

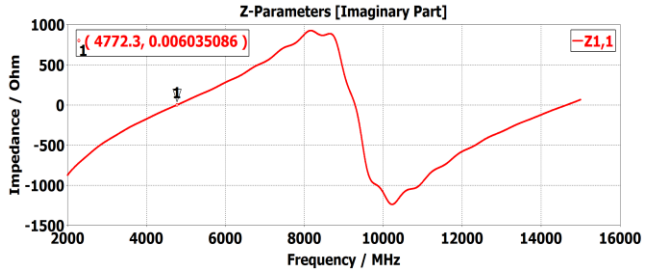

(b)

Fig. 2. Full-wave EM-simulated single dipole. (a) Modeled 30 mm dipole in air. (b) Imaginary part of the input impedance of the dipole.

TABLE I

CALCULATED STANDING WAVE RESONANT FREQUENCIES

Mode (lmn)	f(GHz)	Mode (lmn)	f(GHz)	Mode (lmn)	f(GHz)
110	1.035	330	3.015	530	4.238
210	1.622	420	3.244	350	4.297
120	1.650	240	3.301	610	4.390
220	2.070	430	3.644	101	4.470
310	2.287	340	3.674	011	4.473
130	2.341	510	3.681	160	4.513
320	2.624	150	3.782	111	4.531
230	2.653	520	3.899	620	4.571
410	2.978	250	3.983	201	4.641
140	3.056	440	4.140	021	4.655

have a first resonant frequency closer to 0.48 λ [11]. To verify this, the above-mentioned 30 mm dipole is simulated (being excited by a 1 V Gaussian excitation signal, through a 50 Ohm discrete S-parameter port at the dipole center) in free space with a full-wave EM time domain solver (Fig. 2(a)). To reduce the influence of the dipole thickness, the thickness was set to "infinitely thin". For the 30 mm dipole, its theoretical first resonant frequency should be around 4.796 GHz (0.48 λ), which is verified by the simulated result (shown in Fig. 2(b)). In Fig. 2(b), the imaginary part of the dipole impedance is shown. As discussed above, since the resonant frequency is a frequency at which the dipole has zero imaginary impedance, it can be found that the first resonant frequency of the dipole is about 4.773 GHz, which is very close to the ideal value (4.796 GHz).

B. Box resonance

The box resonances refer here to the standing wave resonances that can exist in the fully closed metallic box. The frequencies at which such standing wave resonances exist can be calculated by [12]:

$$f = \left(\frac{c}{2\sqrt{\varepsilon_r \mu_r}}\right)\sqrt{\left(\frac{l}{a}\right)^2 + \left(\frac{m}{b}\right)^2 + \left(\frac{n}{d}\right)^2} \qquad (1)$$

Here, f is the resonant frequency, c is speed-of-light in air, ε_r and μ_r are the relative permittivity and permeability, respectively. The mode index of each resonance is indicated by l, m and n (all are integer numbers while at least two of them should be non-zero [13]) along the x, y and z axes, respectively. Further, a, b and d represent the corresponding dimensions along these three directions (as indicated in Fig.

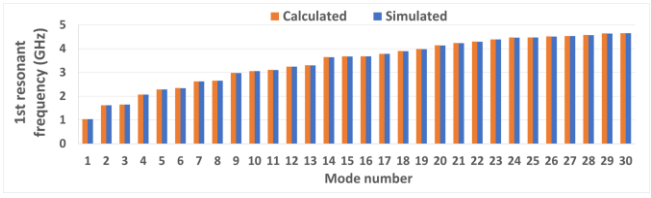

(a)

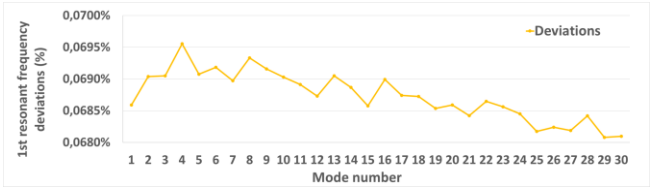

(b)

Fig. 3. Comparison of calculated and simulated resonant frequencies (a) Absolute frequencies (b) Frequency deviations.

1). Table 1 lists the lowest resonant frequencies and their corresponding resonance mode indexes in the fully closed metallic enclosure with the dimensions given in Fig. 1.

Similar to the case of dipole resonance, these theoretical results were verified with simulations with a full-wave eigenmode solver. This comparison is shown in Fig. 3. The maximum difference between the analytically calculated and simulated results is less than 0.07%.

It is worth noting that from equation (1) it can also be concluded that, if keeping other parameters constant, the frequency of each resonance mode will decrease when the dimensions of the box increase. This will be further used in Section III.

III. RESONANCE INTERACTIONS

Now that the dipole and box resonances have been analyzed and verified, their interactions can be investigated by putting the dipole into the closed metallic box. For the convenience of the further analysis, the dipole is located exactly at the center of the box.

First of all, it was investigated if the resonant frequencies of the combined structure are simply the "combination" of the resonant frequencies of the two separate parts. Therefore, in the combined structure, both the first resonant frequency (4.773 GHz) of the dipole (analyzed and simulated in Section II.A) and all the possible box resonances that related to the box (Section II.B) were expected to be found.

The combined structure was simulated again with the full-wave EM time domain solver and the new results are compared with those of the stand-alone dipole and box in Fig. 4. From the results in Fig. 4, the first resonant frequency of the dipole cannot be found, which indicates that the assumption

(a)	(b)
Mode 1 : 1034.4068	Mode 1 : 1034.4068
Mode 2 : 1621.1196	Mode 2 : 1621.1195
Mode 3 : 1649.8363	Mode 3 : 1649.8361
Mode 4 : 2068.8143	Mode 4 : 2068.8143
Mode 5 : 2285.7716	Mode 5 : 2285.7712
Mode 6 : 2339.9221	Mode 6 : 2339.9217
Mode 7 : 2622.3502	Mode 7 : 2622.3493
Mode 8 : 2652.0318	Mode 8 : 2652.0306
Mode 9 : 2976.6053	Mode 9 : 2976.6044
Mode 10 : 3054.4786	Mode 10 : 3054.4757
Mode 11 : 3103.226	Mode 11 : 3103.2255
Mode 12 : 3242.2456	Mode 12 : 3242.2426
Mode 13 : 3299.6796	Mode 13 : 3299.6772
Mode 14 : 3642.1796	Mode 14 : 3642.1763
Mode 15 : 3672.1454	Mode 15 : 3672.1413
Mode 16 : 3678.9056	Mode 16 : 3678.9015
Mode 17 : 3779.6579	Mode 17 : 3779.6566
Mode 18 : 3896.9652	Mode 18 : 3896.9614
Mode 19 : 3980.4372	Mode 19 : 3980.4328
Mode 20 : 4137.6499	Mode 20 : 4098.889
Mode 21 : 4235.5284	Mode 21 : 4137.6462
Mode 22 : 4294.2616	Mode 22 : 4235.5202
Mode 23 : 4387.1759	Mode 23 : 4294.2538
Mode 24 : 4467.2796	Mode 24 : 4387.1729
Mode 25 : 4470.7819	Mode 25 : 4467.2586
Mode 26 : 4510.3463	Mode 26 : 4510.3404
Mode 27 : 4528.4956	Mode 27 : 4528.2553
Mode 28 : 4528.498	Mode 28 : 4528.5061

Fig. 4. Comparison of resonant frequencies with/without dipole. (a) Empty box (without dipole). (b) Box with dipole (along *x*-axis).

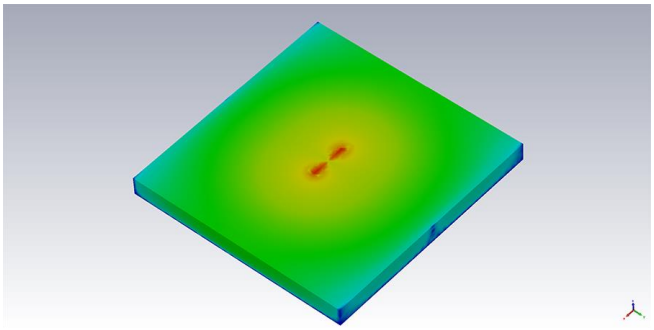

(a)

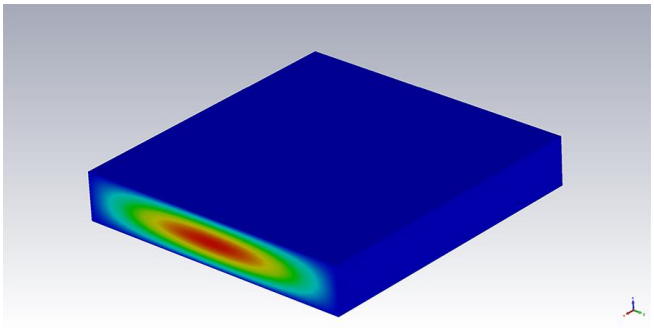

(b)

Fig. 5. E-field patterns of 4.098 GHz and 4.47 GHz. (a) 4.098 GHz. (b) 4.47 GHz.

of "independence" is incorrect. Instead, two special frequencies can be noticed: 4.098 GHz and 4.47 GHz (marked in red). By further checking their E-field patterns in Fig. 5, two particular findings are obtained which do not immediately link with general intuition. The first one is that the first resonant frequency of the dipole is found around 4.098 GHz rather than at the expected 4.773 GHz (hereafter referred to as "Q1"). Indeed, Fig. 5(a) confirms that this frequency is caused by the dipole, not by the box, the other one is that the resonance at 4.47 GHz (one of the original standing wave resonance) disappears (hereafter referred to as "Q2"). Note that, due to the simulation deviation, this simulated 4.47 GHz resonance actually corresponds to the 4.473 GHz resonance in the analytical calculations.

To investigate the above two findings, several assumptions were explored. For Q1, since the shift of first resonant frequency of the dipole took place only after adding the closed metallic box, it is reasonable to assume that there are strong interactions between the dipole and the box, leading to such a significant frequency shift. For Q2, since adding the dipole only resulted in the disappearance of certain resonant frequencies (not all the resonant frequencies) and each box resonance can only exist under certain conditions (e.g., source locations, orientations), it is reasonable to assume that adding the dipole invalidated the boundary conditions of these disappearing box resonances.

To be able to explain the phenomena related to Q1 and Q2, further investigations were done as follows. First, to explain Q1, the dimensions of the box were gradually changed. Instead of changing only one or two dimensions at a time, a parameter named the "scale factor" (sf) was used to simultaneously change all the three dimensions (length, width and height) of the box. As has already been mentioned in Section II.B, the frequency of each resonance mode will decrease with increased box dimensions, which is demonstrated by simulations and shown in Fig. 6. In Fig. 6,

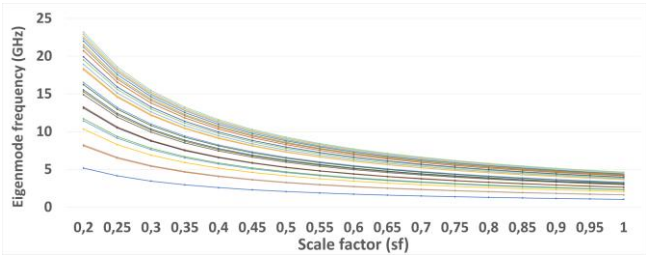

Fig. 6. Frequency of each resonance mode versus box dimension (sf).

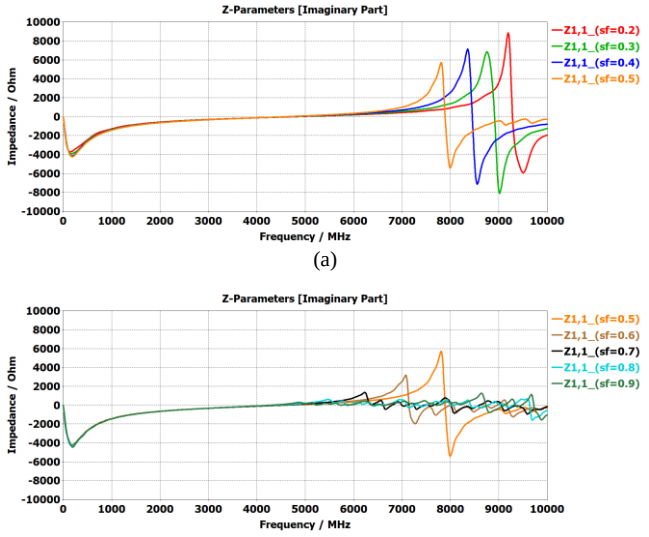

Fig. 7. Imaginary part of the input impedance. (a) sf from 0.2 to 0.5. (b) sf from 0.5 to 0.9.

the *x*-axis and *y*-axis represent the sf and frequency, respectively, while each curve indicates one resonance mode. When gradually changing the sf (*x*-axis) from 0.2 to 1 (sf = 1 represents the original box with the dimensions indicated in Fig. 1), it can be clearly seen that the frequencies of each resonance mode decrease. In addition, the larger the box, the smaller the (frequency) distance between the resonant frequency of the dipole and the enclosure. This behavior makes our analysis of the influence of interaction between the dipole and the enclosure on the resonances more difficult: with the box becoming bigger, all the resonant frequencies related to the box will move closer to the dipole resonance, causing it very hard to pick out the target dipole resonant frequency. Even worse, in Fig. 7 (imaginary part of impedance), when looking at the resonances from the perspective of impedance (as discussed in Section II, resonance happens when the imaginary part of impedance is zero), it is found that with the box becoming bigger (represented by the increase of the sf in the *x*-axis), the resonance modes with higher frequencies can move down and coincide with lower ones, which means the target dipole resonance could be "invisible" by these "coincidences". The above two problems make it almost impossible to directly and clearly analyze what happens in the combined structure. Thus, other solutions have to be found.

Since the box resonances are the main disturbing factors that prevent us from investigating Q1 and answer the question why the dipole resonant frequency is much lower than that in free-space, a new case with only one plate and one dipole (Fig. 8) was proposed. The whole idea is to first decompose the box into metallic plates and then add the plates one by one. By doing this, the possible influences of these plates can be revealed.

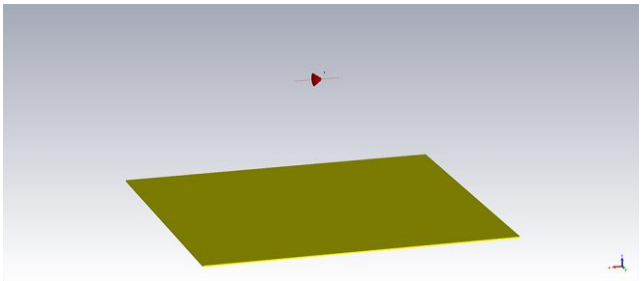

Fig. 8. Case of one dipole above one plate.

In Fig. 8, a dipole is put above one single metallic plate. Note that the dipole could be either parallel or perpendicular to the plate. For simplification purpose, only the configuration of the parallel case is shown in Fig. 8. However, the simulation results for both cases are included in Fig. 9. To further strengthen our analysis, image theory [14] was adopted, which assumes the metallic plate to be infinite. Hence, infinite plates are used in the full-wave solver (also in the following two-plate cases) by correctly setting the corresponding boundaries. The height of the dipole was swept from 2 mm to 100 mm with 2 mm step width. This sweeping operation corresponds to changing the sf in the box case. For the parallel case, height is the distance between the dipole center and the plate while for the perpendicular case, height is the distance between dipole bottom end point and the plate. Since resonances are related to the dipole's input impedance Z_{11}, that input impedance is used here for comparison and analysis. For each height value, the frequency point where the imaginary part of impedance (Z_{11}) first becomes zero is extracted as the first resonant frequency of the dipole. This leads to the relationship between height and corresponding first resonant frequency of the dipole as shown in Fig. 9 (including the perpendicular case).

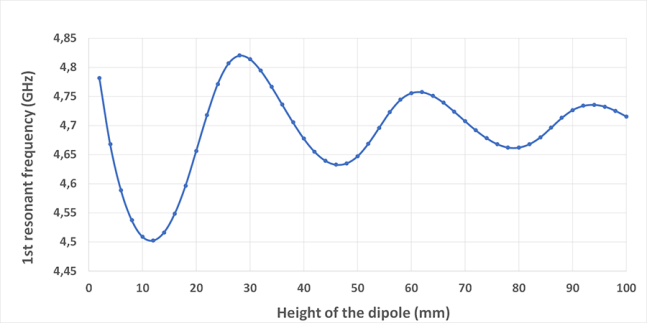

Fig. 9. First resonant frequency versus height in one plate case. (a) Parallel dipole. (b) Perpendicular dipole.

In Fig. 9, when looking at the trend of the first resonant frequency of the dipole with changing height (both parallel and perpendicular cases), it can be seen that the first resonant frequency "oscillates" with the height. However, the plate can only shift the first resonant frequency of the dipole at the low side to around 4.69 GHz which still does not come close to the observed 4.098 GHz in the box resonant frequencies.

In a second step, one more plate was added to the model. Again, for simplification, only the configuration of the case of two parallel plates with a parallel dipole at the center is shown in Fig. 10. The same simulations as in the previous one-plate case were repeated and the results are shown in Fig. 11 (including the perpendicular case). It is worth noting that in the two parallel plates case, "distance" starts from 2 mm while in the two perpendicular plates case, "distance" begins from 32 mm. The reason is that in the perpendicular case, the dipole length (30 mm) should be added to the distance between the two plates. From Fig. 11, it can be clearly seen that the overall trend of the first frequency of the dipole is not as smooth as in the previous case, but it can reach to a larger "oscillation" range and cover the targeted 4.098 GHz (Fig. 11(a)). Specifically, when the height of the dipole above the plate is 17 mm (or the distance between two plates is 34mm, marked in red, corresponding to the sf = 1 case in which dipole is placed at the center of the original box), the first resonant frequency of the dipole is around 4.15 GHz which is already

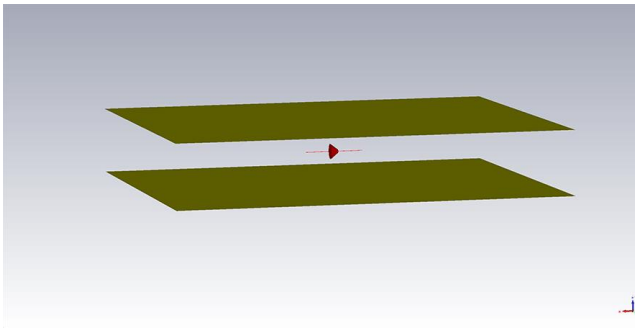

Fig. 10. Case of one dipole with two plates.

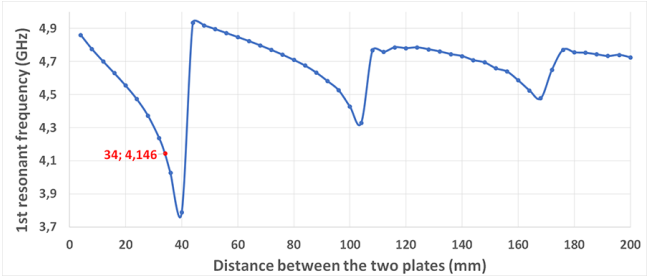

(a)

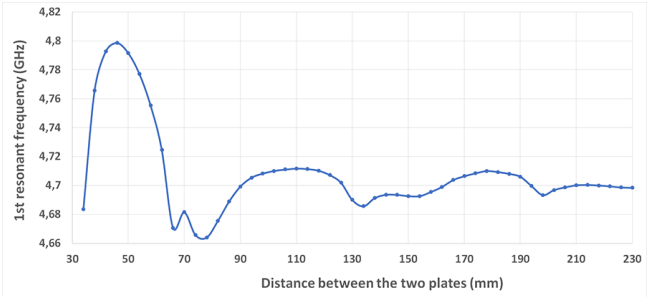

(b)

Fig. 11. First resonant frequency versus height in two plates case. (a) Parallel dipole, (b) Perpendicular dipole.

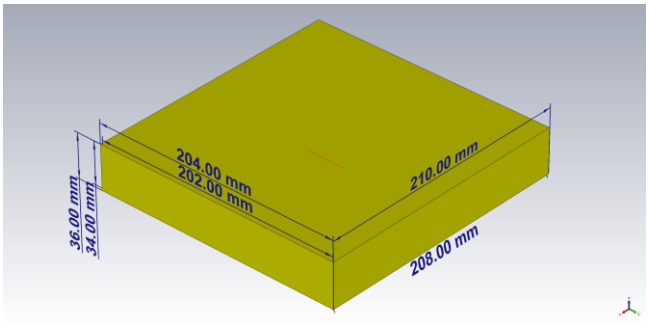

Fig. 12. Closed metallic box with one dipole along *y*-axis.

close to the observed 4.098 GHz. Therefore, it can be speculated that the shift of the first resonant frequency of the dipole is a result of the influence of the metallic plates. The detailed theoretical explanation (including mathematical calculations) and validation work with multiple plates will be performed in the future work.

To explain Q2, again the corresponding E-field pattern was checked. Due to the boundary conditions [15], an EM resonance can only exist when it has at least two components of E_x, E_y, E_z (here only the electric field was considered for simplification). From Fig. 5(b), it can be seen that this 4.47 GHz resonance has E_x and E_z components, which satisfies the above principle. However, when one dipole along *x*-axis was added, this resonance disappeared. Therefore, it can be deduced that this dipole along *x*-axis broke the boundary conditions of the resonance at 4.47 GHz and made this resonance disappear. Then this assumption was verified by changing the orientation of dipole, which is shown in Fig. 12. Instead of along *x*-axis, the dipole was rotated 90 degrees clockwise in the XY-plane to along *y*-axis. Based on this new case, it was expected to see the resonance at 4.47 GHz would

(a)	(b)	(c)
Mode 1 : 1034.4068	Mode 1 : 1034.4068	Mode 1 : 1034.4068
Mode 2 : 1621.1196	Mode 2 : 1621.1195	Mode 2 : 1621.1196
Mode 3 : 1649.8363	Mode 3 : 1649.8361	Mode 3 : 1649.8362
Mode 4 : 2068.8143	Mode 4 : 2068.8143	Mode 4 : 2068.8143
Mode 5 : 2285.7716	Mode 5 : 2285.7712	Mode 5 : 2285.7715
Mode 6 : 2339.9221	Mode 6 : 2339.9217	Mode 6 : 2339.9218
Mode 7 : 2622.3502	Mode 7 : 2622.3493	Mode 7 : 2622.3495
Mode 8 : 2652.0318	Mode 8 : 2652.0306	Mode 8 : 2652.0312
Mode 9 : 2976.6053	Mode 9 : 2976.6044	Mode 9 : 2976.604
Mode 10 : 3054.4786	Mode 10 : 3054.4757	Mode 10 : 3054.478
Mode 11 : 3103.226	Mode 11 : 3103.2255	Mode 11 : 3103.2257
Mode 12 : 3242.2456	Mode 12 : 3242.2426	Mode 12 : 3242.2448
Mode 13 : 3299.6796	Mode 13 : 3299.6772	Mode 13 : 3299.6781
Mode 14 : 3642.1796	Mode 14 : 3642.1763	Mode 14 : 3642.1781
Mode 15 : 3672.1454	Mode 15 : 3672.1413	Mode 15 : 3672.1432
Mode 16 : 3678.9056	Mode 16 : 3678.9015	Mode 16 : 3678.9052
Mode 17 : 3779.6579	Mode 17 : 3779.6566	Mode 17 : 3779.6552
Mode 18 : 3896.9652	Mode 18 : 3896.9614	Mode 18 : 3896.9633
Mode 19 : 3980.4372	Mode 19 : 3980.4328	Mode 19 : 3980.4361
Mode 20 : 4137.6499	Mode 20 : 4098.889	Mode 20 : 4091.3156
Mode 21 : 4235.5284	Mode 21 : 4137.6462	Mode 21 : 4137.6474
Mode 22 : 4294.2616	Mode 22 : 4235.5202	Mode 22 : 4235.5248
Mode 23 : 4387.1759	Mode 23 : 4294.2538	Mode 23 : 4294.2588
Mode 24 : 4467.2796	Mode 24 : 4387.1729	Mode 24 : 4387.1673
Mode 25 : 4470.7819	Mode 25 : 4467.2586	Mode 25 : 4470.747
Mode 26 : 4510.3463	Mode 26 : 4510.3404	Mode 26 : 4510.3407
Mode 27 : 4528.4956	Mode 27 : 4528.2553	Mode 27 : 4527.3377
Mode 28 : 4528.498	Mode 28 : 4528.5061	Mode 28 : 4528.2313

Fig. 13. Closed metallic box with one dipole along y-axis. (a) Empty box. (b) Box with dipole (along x-axis) (c) Box with dipole (along y-axis).

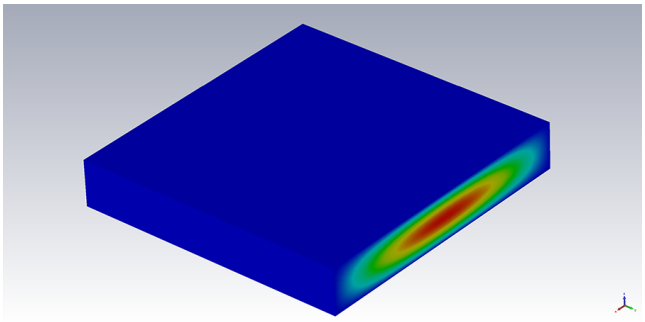

Fig. 14. E-field pattern of 4.467 GHz.

show up again and another resonance which has only E_y and E_z components will disappear. With other conditions and parameters keeping constant, this new case was simulated. From the results in Fig. 13, it can be clearly found that the 4.47 GHz resonance appeared again and another resonance (4.467 GHz) disappeared. By checking the field pattern of this newly disappeared 4.467 GHz resonance (Fig. 14), it was found that this resonance has exact only E_y and E_z components, which confirms our assumption.

IV. Conclusions and Future Work

In this paper, we investigated the influence of the interaction between a dipole and a fully closed metallic box on the dipole's first resonant frequency. After the study of the separate resonances of both dipole and box resonances, the resonances of the overall combined system have been studied. With the help of a full wave time-domain and eigenmode solvers, it is observed that the resonant frequencies of the combined structure are not a simple combination of those of all the separate components. Instead, the combination of all the components can mutually affect the resonant frequencies of separate components by either shifting-, coinciding with-, or removing them. As demonstrated in the paper, shifting or coinciding with the existing resonant frequencies is due to the influence of the surrounding box/plates, while the disappearance of existing resonant frequencies is due to breaking their corresponding boundary conditions.

So, in order to better manage risks in electronic systems with the risk-based approach, the mutual influences between the metallic enclosure and its internal components, as shown in this paper, should be quantified and taken into account in the risk analysis stage and, if necessary, appropriate mitigation measures should be defined.

Our future work will mainly contain the following aspects: first of all, the theoretical explanation of the influence of the plates on the dipole resonant frequencies will be studied and developed. Also, a complete mechanism of the interactions between the metallic enclosure and internal components, as well as between internal components themselves, will be explored, including the theoretical explanation and related validation work. By doing this, more practical solutions for managing the risks caused by such mutual influences can be proposed.

References

[1] A. Degraeve and D. Pissoort, "Study of the effectiveness of spatially EM-diverse redundant systems under plane-wave illumination," in *2016 Asia-Pacific International Symposium on Electromagnetic Compatibility (APEMC)*, Shenzhen, 2016, pp. 211–213.

[2] J. Lannoo, A. Degraeve, D. Vanoost, J. Boydens and D. Pissoort, "Study on the use of different transmission line termination strategies to obtain EMI-diverse redundant systems," in *2018 IEEE International Symposium on Electromagnetic Compatibility and 2018 IEEE Asia-Pacific Symposium on Electromagnetic Compatibility (EMC/APEMC)*, Singapore, 2018, pp. 210-215.

[3] K. Armstrong, "Why increasing immunity test levels is not sufficient for high-reliability and critical equipment." In 2009 IEEE International Symposium on Electromagnetic Compatibility, pp. 30-35..

[4] F. Leferink, J. van der Ven, H. Bergsma and B. van Leersum, "Risk based EMC for complex systems," in *2017 XXXIInd General Assembly and Scientific Symposium of the International Union of Radio Science (URSI GASS)*, Montreal, QC, 2017, pp. 1-4.

[5] "IEEE 1848-2020 - IEEE Standard on Techniques & Measures to Manage Functional Safety and Other Risks With Regard to Electromagnetic Disturbances," Apr. 2020.

[6] F. Leferink, "Risk-based vs Rule-based Electromagnetic Compatibility in Large Installations," in *2018 IEEE 4th Global Electromagnetic Compatibility Conference (GEMCCON)*, Stellenbosch, South Africa, 2018, pp. 1-4.

[7] J. Du, Y. Kim, J. Yook, J. Lee and J. S. Choi, "Coupling effects of incident electromagnetic waves to multilayered PCBs in metallic enclosures," in *2015 International Workshop on Antenna Technology (iWAT)*, Seoul, 2015, pp. 359-361.

[8] B. Nie, P. Xiao and P. Du, "Electromagnetic resonance analysis of a shielding enclosure with apertures excited by a plane wave," in *2018 IEEE International Symposium on Electromagnetic Compatibility and 2018 IEEE Asia-Pacific Symposium on Electromagnetic Compatibility (EMC/APEMC)*, Singapore, 2018, pp. 355-358.

[9] Yingpeng Fan, Zhengwei Du, Ke Gong and Guoding Li, "Analysis on shielding effectiveness of metallic enclosures with slot," in *Asia-Pacific Conference on Environmental Electromagnetics, 2003 (CEEM 2003*), Hangzhou, China, 2003, pp. 43-46.

[10] J. W . Healy, "Antenna here is a Dipole", June 1991, pp. 23-26.

[11] C. A. Balanis. *Antenna theory: analysis and design*. Wiley-Interscience, 2005, pp. 184.

[12] K. Armstrong, "The Physical Basis of EMC," *The EMC Journal*, issue. 85, November 2009, pp. 23–34.

[13] Webb, Andrew. "Cavity-and waveguide-resonators in electron paramagnetic resonance, nuclear magnetic resonance, and magnetic resonance imaging." Progress in nuclear magnetic resonance spectroscopy 83 (2014): 1-20.

[14] C. A. Balanis, *Advanced Engineering Electromagnetics*. Wiley-Interscience, 2012, pp. 315-323.

[15] C. A. Balanis, *Advanced Engineering Electromagnetics*. Wiley-Interscience, 2012, pp. 12-18.